Characterization of Emitted Vibration from Turbo-Brayton Cryocoolers

K. Cragin, K. Rule, M. Zagarola

Creare LLC
Hanover, NH 03755

ABSTRACT

Turbo-Brayton cryocoolers are known for low emitted vibrations due to the lack of reciprocating parts. The only moving parts are the miniature turbomachine rotors which are precisely balanced and operate at extremely high rotational speeds (3000 to 10,000 rev/s are typical). The high operating speed, low rotor mass and low rotor imbalance results in physical displacements of cryocooler components that are on the order of nanometers. The first space implementation of a turbo-Brayton cryocooler was for cooling the NICMOS instrument on the Hubble Space Telescope (HST). On-orbit operations indicated that the cryocooler could not be detected by the super-precise instruments on the HST. Future missions may have more restrictive vibration requirements or different integration approaches than HST and a quantitative assessment of emitted vibration from a turbo-Brayton cryocooler is needed. During the development of the NICMOS cryocooler, several tests were conducted to characterize the emitted vibrations from the cryocooler, but these tests did not produce comprehensive information due to either high background vibrations or non-prototypical operation of the cryocooler. Recent work at Creare has focused on quantifying the emitted vibration of turbo-Brayton cryocooler technology using computational fluid dynamics/structural simulations of representative turbo-Brayton components at prototypical operating conditions. This paper describes the analysis work.

INTRODUCTION

Creare has developed and demonstrated a unique class of mechanical cryocoolers, turbomachine-based reverse-Brayton cryocoolers, which has an inherent advantage over competing active cryocoolers when it comes to vibration emittance. Turbo-Brayton cryocoolers utilize miniature turbomachines to compress and expand the working gas as part of a reverse-Brayton thermodynamic cycle. The only moving parts in these cryocoolers are miniature turbomachine rotors which have masses of 1 to 10 grams. The rotors have diameters of a few millimeters and operate at speeds of several thousand revolutions per second. These small sizes and high speeds are required for high thermodynamic efficiency at the low power levels associated with space cryocooling applications. The rotors are supported on non-contacting gas bearings, and the turbomachines use clearance seals so there is no mechanical contact or wear mechanism during normal operation. Contact between the rotor and bearings occurs briefly during start-up and shutdown operations, but the extremely low contact forces prevent any

Cryocoolers 19, edited by S.D. Miller and R.G. Ross, Jr.

appreciable wear during thousands of start-up and shutdown cycles. Numerous demonstrations support this claim (Breedlove et al. 2001). In addition, the rotors are precisely balanced for high-speed operation, and the cycle gas flow is continuous. The result is that emitted vibrations are extremely small and occur at high frequencies where the predicted mechanical displacement caused by vibrations is on the order of nanometers.

The initial space demonstration of a turbo-Brayton cryocooler occurred during NASA's NICMOS Cooling System (NCS) Program (Swift et al. 2008). The NCS consists of a single-stage turbo-Brayton cryocooler coupled with a cryogenic circulator and capillary pump loop. The system provides 7 W of cooling at 70 K to the NICMOS instrument on the Hubble Space Telescope and replaced the solid nitrogen cryogen that had depleted prematurely after less than two years in space. The NCS was deployed and integrated with NICMOS by astronauts during STS–109 (Space Shuttle Columbia) in March 2002 and operated nearly continuously for more than 6.5 years before a problem with an external cooling loop caused the system to be deactivated.

During the NCS program, several tests were conducted to characterize the emitted vibrations from the cryocooler. The Vibration Emittance Test (VET) described in Clapp et al. (2002) showed continuous performance below the derived maximum Root-Sum Square acceleration allocated to the center of mass for the NCS (4.1 micro-g RMS over the frequency range of 0.001 to 50 Hz). This test was conducted with the compressor in surge and considered by Clapp, et al., to be an upper bound on vibrations expected during steady operation. Unfortunately, no testing was performed at design operating conditions. Even at this off-design condition, measured vibrations (3.5 mas jitter) were well below the required budget for the Hubble Space Telescope of 7.7 mas jitter. Additional test data were obtained during the servicing mission to the Hubble Space Telescope responsible for the installation of the NCS. During that mission (Hubble Servicing Mission 3B), measured jitter was recorded during cooldown (surge) as 0.9 mas. It is worth noting that at steady-state temperatures, Clapp (2003) reports no measureable jitter from the NCS.

Future missions may have more restrictive vibration requirements or different integration approaches than HST and a quantitative assessment of emitted vibration from a turbo-Brayton cryocooler is needed. Recent work at Creare has focused on quantifying the emitted vibration of turbo-Brayton cryocooler technology using two approaches. The first approach utilizes computational fluid dynamics/structural simulations, and will be the subject of this paper. The second approach involves testing the vibration emitted and will be the subject of a future paper.

VIBRATION SOURCES

Unlike Stirling and pulse tube cryocooler systems, the fundamental operating frequencies for turbo-Brayton cryocoolers are well above vibration harmonics that excite spacecraft resonant frequencies (Ross 2003). The high operating frequencies make turbo-Brayton cryocoolers ideal for space telescopes requiring high pointing accuracy. The primary vibration sources of concern for a turbo-Brayton cryocooler are described below.

Rotor Mass Imbalance

Emitted vibration from rotor motion at steady state is caused by synchronous imbalance of the rotor and sub-synchronous rotor whirl. Synchronous imbalance is a lateral motion of the rotor within the hydrodynamic bearing clearance that occurs as a result of mass imbalance in the shaft/impeller. In this case, emitted vibrations occur at the same frequency as the shaft rotational speed. These resulting forces are emitted at frequencies that are expected to be well above structural resonances of most payloads and should not affect pointing accuracy. Rotor whirl occurs at resonant frequencies for the rotor and bearings. By design, these frequencies are below the rotational speed of the shaft. We have observed rotor whirl to be greater than 1 kHz for rotor operating speeds of greater than 3,000 rev/s.

Turbomachine-Fluid Interaction

The primary flow interaction between the turbomachines and the balance of the fluid volume that has the potential to emit forces is compressor surge. Surge occurs when there is a mismatch between the compressor head-flow characteristics and the flow resistance of the cryocooler flow loop, which is dominated by the flow resistance of the turbine. High loop flow resistance causes separation and reversed flow inside the compressor impeller resulting in unsteady flow and significant pressure fluctuations that produce detectible vibration. For our turbo-Brayton cryocoolers, surge only occurs during cooldown when the compressor flow rate is low due to high flow resistance at the turbine. Decreasing cold-end temperature during cooldown reduces turbine flow resistance and relieves surge. Prior testing of the NCS has characterized the measured vibration levels during surge to be in the 10's of mN at frequencies of 0.1 to 10 Hz. Because surge will not be present during steady-state operation of the cryocooler, no further analysis is presented here.

Flow Induced Forces

Lower frequency vibration in the cryocooler system can be caused by flow-induced pressure fluctuations in the cryocooler tubing, load heat exchangers, and auxiliary components. Two mechanisms contribute to flow induced vibration—vortex shedding and flow turbulence. Vortex shedding is an oscillating flow condition that can occur in a flow when the fluid passes over a bluff body. Abrupt changes in passage geometry can also result in vortex shedding, such as flow discharge into a plenum or through an internal restriction. The vortex shedding frequency can be approximated via an appropriate Strouhal number, defined as:

$$St = \frac{fL_{char}}{V_{avg}} \tag{1}$$

where f is the vortex shedding frequency (Hz), L_{char} is the characteristic length of an obstruction, and V_{avg} is the average flow velocity. The second mechanism, flow turbulence, is characterized by a much broader frequency range than is typical of vortex shedding. These fluctuations are random in nature and can produce a net force through RMS velocity fluctuations accompanied by pressure fluctuations in the flow.

We utilized Fluent® to assess the turbulent eddies and vortices inside representative flow passage geometries for the cryocooler. We can bound the exported RMS force magnitude by evaluating the integrated pressure force along the tube wall. The turbulence was not modelled at all length scales, but rather, we utilized a Large Eddy Simulation (LES) (Pope 2000; Sagaut 2006; Leonard 1974), which accurately and directly computes the energy containing turbulent flow scales and incorporates a turbulence model to include the effect of the small flow scales that have negligible contribution to the overall turbulent kinetic energy. This approach strikes a balance between accuracy and computational time.

COMPRESSOR AND TURBOALTERNATOR VIBRATION ANALYSIS

The two primary factors associated with emitted vibration in the compressor and turboalternator are synchronous imbalance of the rotating shaft and sub-synchronous whirl. The characteristic frequency of synchronous imbalance is equal to the rotational frequency of the system (3000 to 10,000 rev/s are typical). The shaft and bearing system can be modeled as a simple mass-spring system. Based on observed runout, typical rotor masses and typical speeds, the forces transmitted to the turbomachine housings are on the order of 1 to 2 N and occur at frequencies greater than 3000 Hz, which will have negligible impact on jitter due to the high frequency.

In addition to synchronous imbalance, rotor induced vibration is possible at lower rotational frequencies as a result of rotor whirl. During component-level testing of each turbomachine, operation is verified and bearing clearances are adjusted to operate without detectible whirl, so this source of vibration is not expected to be present in the cryocooler.

FLOW-INDUCED VIBRATION ANALYSIS

To determine the magnitude of emitted vibration from flow disturbances, we utilized the turbulence modeling capabilities in Fluent. We analyzed representative components in the cryocooler to obtain a bounding estimate of flow-induced vibration, and assumed that the effects of flow coupling between subsections are negligible relative to the magnitude of flow induced noise within each analysis region. The three items assessed were: 1) abrupt changes in flow passage geometry of interconnecting tubing between components representing a weld penetration or step; 2) small radius bends in the interconnecting tubing; and 3) flow entering and exiting the load heat exchangers. The predicted RMS force magnitude for each geometry and flow condition analyzed is summarized in Table 1. The details of the analysis are given below.

Modeling Approach

The LES turbulence simulations used to produce the results in the subsequent sections were found to be very computationally intensive. One of the major downsides of LES results from the presence of boundaries where the dynamically important turbulent eddies are very small. The size of the turbulent eddies scales with flow Reynolds number. As the Reynolds number increases, the size of the viscous sublayer decreases, along with the near wall turbulence length scales. To accurately model the boundary layer in LES, one must use a very fine mesh resolution in the near wall region.

One option to overcome the difficulties with mesh size at high flow Reynolds numbers is to utilize a suitable eddy-viscosity model to separately model the inner part of the logarithmic boundary layer (Davidson 2004). This was accomplished in Fluent by utilizing an algebraic Wall Modeled Large Eddy Simulation (WMLES). Here, the effects of small energy containing eddies near the wall are captured using a Reynolds Averaged Navier Stokes (RANS) model. The outer portion of the boundary layer, which contains the largest eddies, is directly modeled using LES.

To assess the impact of the WMLES approach on model accuracy, we can examine the energy content associated with the small eddies (which are simulated with RANS) versus the large scale eddies (which are directly modeled). Figure 1 illustrates the distribution of kinetic energy as a function of turbulent eddy size. We can see that the majority of energy is contained within the largest scale eddies. The energy content decreases with eddy size down to the approximate limit of the smallest eddy size in the flow (the Kolmogorov microscale, η).

While WMLES is largely Reynolds number independent for channel and pipe flows, the computational cost increase relative to a RANS models is still high (Menter 2012). Progressing solutions out to reasonable flow periods for these analyses necessitated the use of dedicated computing resources. Furthermore, a comprehensive time step and mesh resolution study was required to ensure that proper results were being generated.

Table 1. Flow induced vibration analysis summary.

Geometry	Analysis Case	Temp. (K)	Pressure (kPa)	Sample Period (s)	RMS Emitted Force (mN)	Frequency for Maximum Force (Hz)
Weld-in-tube	1	320	209.6	0.4	0.012	20.0
	2	85	324.7	0.4	0.013	52.2
90 Degree Tube Bend	3	320	209.6	0.4	0.173	22.5
	4	85	324.7	0.4	0.030	145.0
IFHX Inlet Section	5	85	324.7	0.35	1.285	74.3
IFHX Outlet Section	6	85	324.7	0.4	1.758	75.0

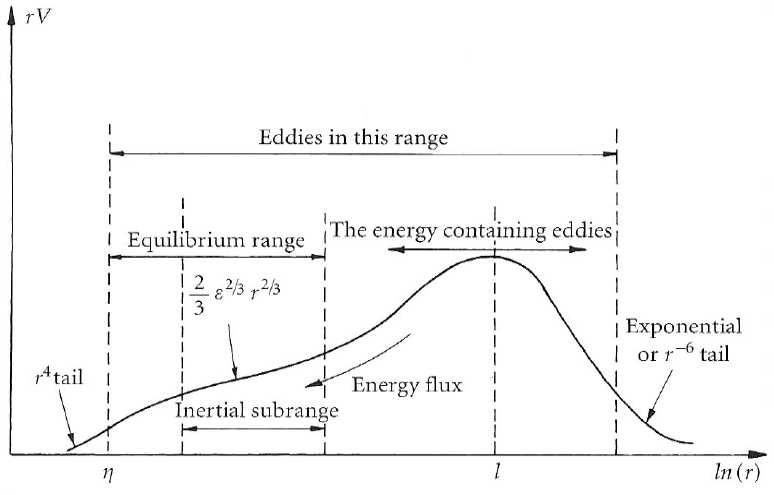

Figure 1. Distribution of turbulent kinetic energy as a function of eddy size (General Shapes per Davidson 2004). Here l is the size of the large, energy-containing eddies in the flow and η represents the approximate lower limit on eddy size.

Vibration Analysis Setup and Results

As a baseline analysis, we considered a weld projection in the ID of the cold- and warm-end tubing. To estimate the ID at the weld location, we examined welded tube joints with the same tube OD (0.5 in.) as typically used in our cryocoolers. We used a worst-case weld penetration thickness of 0.16 in. for this analysis, restricting the available flow area by 13%.

We analyzed two gas flow conditions as bounding cases for this investigation. The first condition corresponds to an upper limit on the flow velocity in the cryocooler, with the fluid at the warm-end temperature and compressor inlet pressure (Case 1). For the second analysis, (Case 2) we roughly doubled the flow's Reynolds number, consistent with flow conditions at the cold end of the cryocooler. We selected a tube length upstream and downstream of the internal weld based on an analytical correlation of the hydrodynamic development length for turbulent flow provided in Nellis and Klein (2009). This value also set the analysis region for flow induced vibration downstream of the weld. A visual representation of the flow field downstream of the weld feature is shown in Fig. 2. We can clearly see an area of flow separation resulting from the step change in passage diameter after the weld. Coherent flow structures appear in the near wall region (colored in blue) and dissipate as we move further downstream.

We calculated the integrated radial force downstream of the weld feature at each time step in Fluent by summing the dot product of the pressure force vector on the interior wall face with a unit vector in the y and z directions (Fig. 2). Figure 3 shows the force for Case 1 for a flow period of 0.4 s. We can combine the results from these two orthogonal directions at each time step to assess the magnitude of the greatest wall-normal force. We utilized post-processing code in MATLAB® to resolve spectral content over the analysis period (Fig. 4). The falloff in magnitude at high frequencies should follow a power law with a negative exponent according to turbulence theory (Pope 2000). We see that the forces predicted by the LES simulation are dominated by broadband turbulence. Furthermore, we do not observe any significant contribution to emitted force from vortex shedding, which would appear as a large increase in force magnitude at a single frequency. The emitted force predicted in ANSYS® is very small, on the order of 0.012 mN RMS.

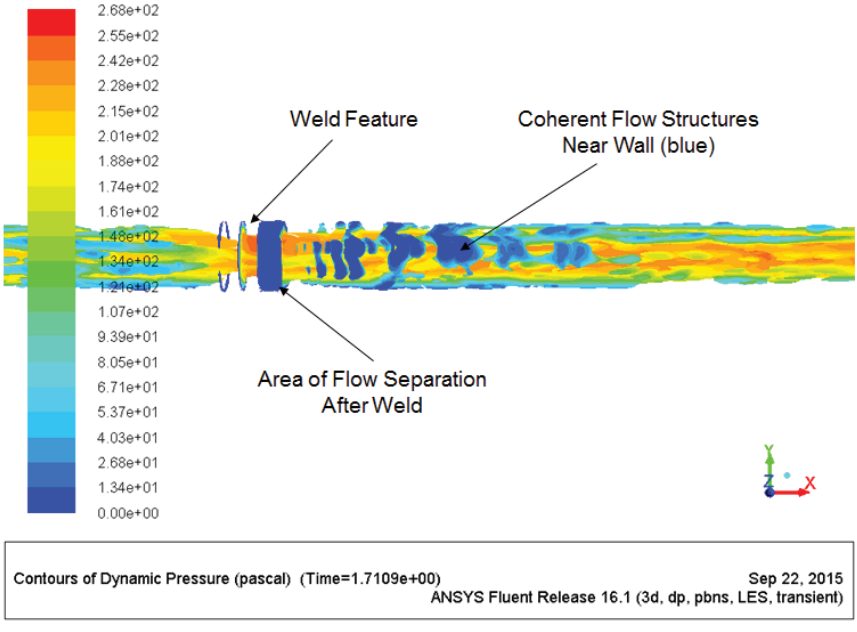

Figure 2. 3-D Flow field downstream of the weld feature. Results are shown for analysis Case 1.

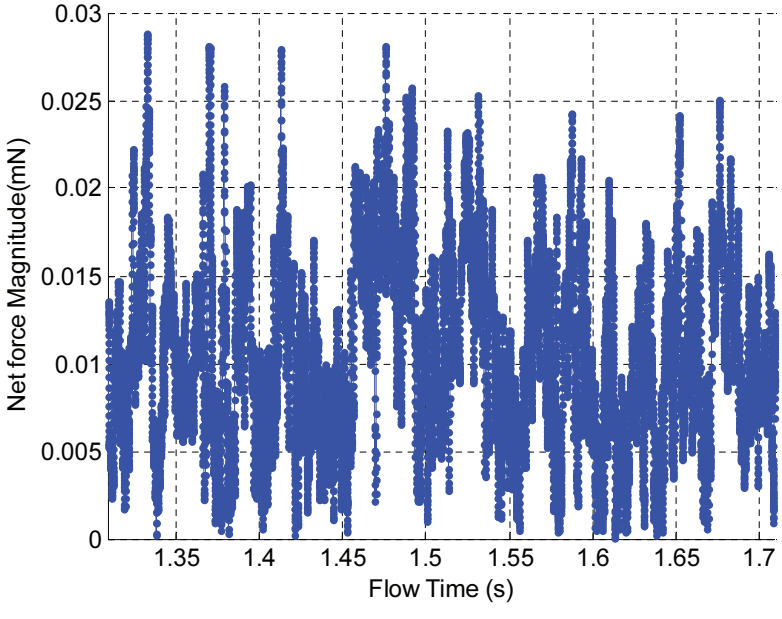

Figure 3. Net force magnitude on the interior tube wall downstream of the weld feature as a function of flow time. Results are shown for a flow period of 0.4 s for analysis Case 1.

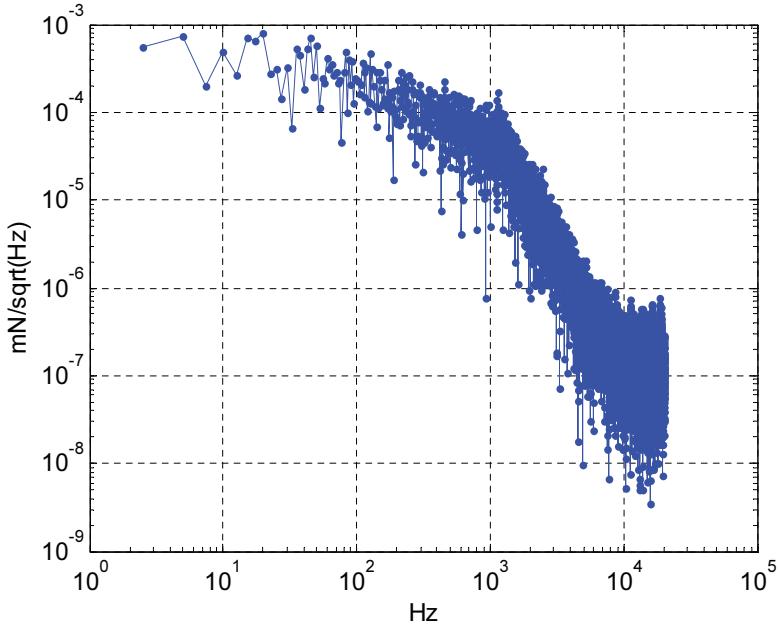

Figure 4. Spectral analysis of wall-normal force magnitude for the weld-in-tube flow geometry. Results are shown for analysis Case 1.

Results Summary

We repeated the vibration analysis for the additional five cases given in Table 1. Each analysis case required several weeks of computational time on a high-performance parallel computer cluster. The spectral results for each case are plotted in Fig. 5. We see that the IFHX remains the dominant contributor at frequencies up to 1 kHz. Flow induced vibrations are dominated by broadband-turbulence for every case considered.

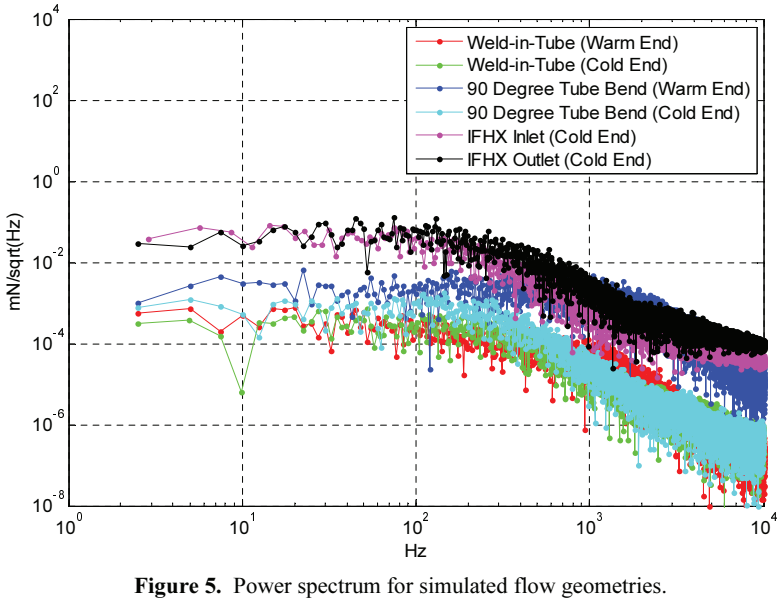

Figure 5. Power spectrum for simulated flow geometries.

CONCLUSIONS AND FUTURE WORK

The primary objective of this analysis is to quantify limits for emitted vibration from a turbo-Brayton cryocooler. For the compressor and turboalternator, we have shown a conservative emitted disturbance on the order of 1 N due to mass imbalance at frequencies greater than 3 kHz. Forces resulting from sub-synchronous rotor whirl will be of the same order of magnitude and have been shown to occur experimentally at frequencies 25 to 35% of the rotating speed at steady state (greater than 1 kHz for operating speeds above 3,000 Hz). The high frequency of these forces results in imperceptible vibrations of the turbomachines.

Using Fluent, we demonstrated an approach to assess turbulence and flow noise in the interconnecting tubing and load heat exchangers and performed an analysis to quantify the magnitude of flow induced vibrations on interior surfaces of the cryocooler flow loop. We examined three key flow geometries for the cryocooler assembly including a straight section of tubing with an over-penetrated weld joint, a small radius 90 degree tube bend, and the inlet and outlet sections of the load heat exchanger. We found that vibrations produced by broadband turbulence dominate in these sections of the cryocooler assembly. Results from these analyses can be imported into a structural harmonic analysis to predict the actual emitted disturbance for a specific payload.

The outlet section of the IFHX remains the largest contributor of flow induced vibrations. We predicted a worst-case RMS force of 1.76 mN for this geometry. No attempt was made to redesign the load heat exchanger to reduce the emitted forces at this location.

Future work involves measuring the emitted vibration of representative turbo-Brayton cryocooler components at prototypical operating conditions. This work is planned to be performed at the Cryocooler Vibration Output Test Facility that was developed and is operated by the Aerospace Corporation.

ACKNOWLEDGEMENTS

We gratefully acknowledge NASA for their support of this work on Contract NNX14CG57C.

REFERENCES

1. Breedlove, J.J., Zagarola, M.V., Nellis, G.F., Gibbon, J.A., Dolan, F.X. and Swift, W.L., “Life and Reliability Characteristics of Turbo-Brayton Coolers,” *Cryocoolers 11*, edited by R.G. Ross, Jr., New York, NY, Kluwer Academic/Plenum Publishers (2001), pp. 489-498.
2. Clapp, B.R., “Vehicle Disturbance Test Report for SMOV-3A/B,” Mission Operations, System Engineering & Software Program Engineering Memorandum, EM MOSES 1226, Mar 31, 2003.
3. Clapp, B.R., Stills, J.W. and Voorhees, C.R., “Hubble Space Telescope Pointing Performance Due to Micro Dynamic Disturbances from the NICMOS Cryogenic Cooler,” AIAA 2002-1249 (2002).
4. Davidson, P.A., *Turbulence: An Introduction for Scientists and Engineers*, New Yord: Oxford University Press (2004).
5. Leonard, A., “Energy Cascade in Large-Eddy Simulations of Turbulent Fluid Flows,” *Advances in Geophysics A*, vol. 18 (1974), pp. 237-248.
6. Menter, F.R., *Best Practice: Scale-Resolving Simulations in ANSYS CFD*, ANSYS, Inc. (2012).
7. Nellis, G. and Klein, S., *Heat Transfer*, Cambridge University Press (2009).
8. Pope, S., *Turbulent Flows*, Cambridge University Press (2000).
9. Ross, R. G., “Vibration Suppression of Advanced Space Cryocoolers – an Overview,” Presented at the International Society of Optical Engineering (SPIE), Mar 2-6, 2003.
10. Sagaut, P., *Large Eddy Simulation for Incompressible Flows,* Springer (2006).
11. Swift, W.L., Dolan, F.X. and Zagarola, M.V., “The NICMOS Cooling System – 5 Years of Successful On Orbit Operation,” *Trans. of the Cryogenic Engineering Conference—CEC*, vol. 53, edited by J.G. Weisend II (2008), pp. 799-806.